Artificial envelopment of nonenveloped viruses: enhancing adenovirus tumor targeting *in vivo*

Ravi Singh, Bowen Tian, and Kostas Kostarelos[1]

Nanomedicine Laboratory, Centre for Drug Delivery Research, The School of Pharmacy, University of London, London, UK

ABSTRACT **Recombinant adenovirus (Ad) is a powerful tool in gene therapy. However, the ability to deliver Ad by systemic administration is limited due to rapid clearance from blood circulation, transfection of nontarget tissues, toxicity, and immunogenicity. To address these limitations, we developed an artificially enveloped Ad vector prepared by self-assembly of lipid bilayers around the Ad capsid. The physicochemical and structural features of the enveloped Ad vector can be altered according to the type of lipid used without the need for genetic modification or conjugation chemistry. Here we engineered 4 different types of artificially enveloped Ad using cationic, neutral, fusogenic, and PEGylated lipids to form the envelopes and obtained extended blood circulation times following i.v. administration and reduced vector immunogenicity. Moreover, the PEGylated lipid-enveloped Ad was capable of specifically delivering genes *via* the systemic circulation to solid tumors subcutaneously implanted in the absence of high levels of gene transfer to the liver and spleen. This provides the basis for the development of a novel vector platform for systemic delivery of Ad to disseminated targets. Furthermore, the artificial envelopment of Ad presented herein is an illustration of a general strategy to modulate the biological function of nonenveloped viruses and may have implications broader than gene therapy.—Singh, R., Tian, B., Kostarelos, K. Artificial envelopment of nonenveloped viruses: enhancing adenovirus tumor targeting *in vivo*. *FASEB J.* 22, 3389–3402 (2008)**

Key Words: gene therapy · liposome · cancer · nanoengineering · immunology · nanomedicine

Recombinant adenovirus (Ad) vectors have been applied, with promising results, to the treatment of cancers resistant to established therapies (1–5). However, current clinical treatment is limited to localized delivery to solid tumors by intratumoral administration and is hampered by a multitude of problems, including poor dissemination into the tumor mass, variability of administration, and inability to access deep-seated tumors. As most cancer deaths involve disseminated disease, it is necessary to develop blood-borne therapeutics to target cancer cells throughout the body. There remain many limits on the ability to effectively deliver Ad into the systemic circulation. These include vector immunogenicity, toxicity, and accumulation in nontarget tissue, especially the liver (6). Furthermore, it is believed that low-level expression of the coxsackie and adenovirus receptor (CAR) on tumor cells may be the rate-limiting factor for infectivity of Ad vectors (7). Ad is cleared from the bloodstream extremely rapidly, primarily by tissue macrophages (8, 9), with a blood circulation half-life of ~2 min in mice (10), giving little window for targeting of tumor cells.

To address these issues, numerous strategies have been developed to modify adenoviral tropism and to reduce vector-related toxicity. Such strategies often involve complex genetic modifications of the Ad (11–13), the introduction of a linker molecule conjugated onto the viral surface (14–16), or chemical modification of the viral capsid (17–19). None of these strategies have proven effective for targeting the Ad to tumor tissue *in vivo*, and many introduce potentially new problems including low production efficiency, reduction of vector function, difficulties in purification, and lack of vector stability. Creation of an Ad vector with enhanced tumor targeting necessitates extending blood circulation time, allowing the vector to accumulate in tumor sites after escaping from the systemic circulation into tumors through the fenestated vasculature common to many cancers (20, 21). Interactions between the Ad capsid with serum and various cell types lead to its rapid blood clearance, and therefore the viral components responsible for native tropism need to be masked or ablated to achieve a stealth effect. At least 3 capsid domains determine native viral tropism: the fiber knob, which binds to CAR (22); the Arg-Gly-Asp (RGD) domain of the penton base, which binds to $\alpha v\beta 5$ integrins (23); and the fiber shaft, which binds heparin sulfate proteoglycan receptors (24). In mice, the binding of Ad hexon to coagulation factor X recently has been demonstrated to be responsible for infection of the liver following intravenous injection (25). Though

[1] Correspondence: Nanomedicine Laboratory, Centre for Drug Delivery Research, The School of Pharmacy, University of London, 29–39 Brunswick Sq., London WC1N 1AX, UK. E-mail: kostas.kostarelos@pharmacy.ac.uk

doi: 10.1096/fj.08-103275

numerous attempts have been made to alter vector biodistribution through modification of these domains, the problem of liver tropism has proven difficult to overcome, with only modest increases in blood circulation time observed for penton/fiber ablated vectors (12).

Ad capsid proteins are also highly immunogenic and are responsible for most of the antigen-specific immunity. It has been demonstrated that encapsulation of Ad in alginate or chitosan nanoparticles greatly reduces its immunogenicity (26), but these systems are more suitable for local delivery as they are far larger than the nanoscale dimensions (<200 nm in mean diameter) required for effective systemic delivery. Formation of complexes by mixing Ad with cationic liposomes has been demonstrated to broaden vector tropism (27–29), improve Ad transfectivity in the presence of neutralizing immunity (30, 31), and alter vector biodistribution *in vivo* (32). However, these vectors are prone to aggregation, leading to widely variable and inherently unstable complexes that are difficult to translate to a clinical setting. Alternatively, numerous reports have demonstrated the feasibility of using polymers to mask the surface of the Ad, leading to reduced immunogenicity and, most important, extending blood circulation times (19, 33, 34). Use of these techniques requires irreversible alteration of Ad surface characteristics, which can affect vector function. In addition, such vectors are difficult to produce at high titers and to purify following polymer conjugation. Although one report demonstrates the possibility of using polymer-coated Ad for tumor targeting (35), there is little room for readily tailoring vector surface characteristics to specific applications following such conjugation strategies.

Here, we have engineered an artificially enveloped Ad vector to reduce the interaction of the viral capsid with cellular and blood components. This vector can be built using self-assembly principles without the need for manipulation of the Ad genome or covalent conjugation to the viral capsid, as described elsewhere (36). We hypothesized that a lipid-enveloped Ad would have novel biological properties determined by the type of lipids used to construct the artificial envelope. Alteration of the lipid components and optimization of physicochemical properties would allow for targeting of the vector to different tissues *in vivo*. Inclusion of stealth components like PEG-lipids in the envelope may extend plasma circulation time and lead to accumulation of the vector in cancer tissue. In the present study, we provide evidence that Ad vectors wrapped with artificial envelopes can be tailored to preferentially accumulate and express genes in tumor tissue with little interaction with nontarget tissue *in vivo*. Further, we offer a proof-of-principle demonstration that these vectors are less immunogenic than normal Ad vectors.

MATERIALS AND METHODS

Viral vectors

Recombinant Ad type 5 was purchased from the Baylor College of Medicine Vector Development Laboratory (Houston, TX, USA). For these studies, we used the vector Ad.βgal, encoding for the beta-galactosidase reporter gene driven by the cytomegalovirus promoter and Ad.Null, with an empty expression cassette. Stocks were stored at −80°C in glycerol buffer at a concentration of 5×10^{12} particle units (pu)/ml until ready for use.

Preparation of lipid-enveloped Ad

Dimyristoyl phosphatidylcholine (DMPC) and cholesterol (Chol) were purchased from Sigma-Aldrich (Gillingham, UK). DOTAP [(1,2-dioleoyloxypropyl)-*N,N,N*-trimethylammonium chloride], 1,2-dioleoyl-sn-glycero-3-phosphoethanolamine (DOPE), and 1,2-distearoyl-sn-glycero-3-phosphoethanolamine-*N*-[methoxy(polyethylene glycol)-2000] (DSPE-PEG_{2000}) were purchased from Avanti Polar Lipids (Alabaster, AL, USA). DMPC:Chol at a 2:1 M ratio, DOTAP:Chol at a 2:1 M ratio, or DOTAP:DOPE:DSPE-PEG_{2000} at a 1:8:1 M ratio, and DMPC:Chol:DSPE-PEG_{2000} at a 2:1:0.1 M ratio were dissolved in 4:1 (vol:vol) chloroform:methanol (both from Sigma-Aldrich) in a 25 ml round-bottom flask. A lipid film was formed using a rotovaporator (Büchi, Flawil, Switzerland). After 1 h under a vacuum, the film was further dried for 15 min under a nitrogen gas stream. Ad stock was thawed, then diluted in 1 ml distilled water with 5% dextrose (D5W), then added to the flask to hydrate the film. To ensure thorough hydration, a small magnetic stirring bar (10 mm) was added, and the hydrating films were stirred for 30 min at room temperature. The stirrer was removed, and the flask was then placed in an ultrasonic water bath (VWR Model 300TH; VWR, Lutterworth, UK) for 15 min at 30°C. The enveloped virus suspensions were transferred to microcentrifuge tubes and placed at room temperature for 3 h to allow the envelopes to stabilize. Unless otherwise noted, fresh vectors were prepared for all experiments.

Artificially enveloped Ad dynamic light scattering

All measurements were made using the Zetasizer Nano ZS (Malvern Instruments, Malvern, UK). For determination of the hydrodynamic diameter of enveloped Ad, vectors were prepared as described above and diluted 10-fold in D5W. Size and zeta potential analyses of Ad alone were conducted at an Ad concentration of 5×10^{10} pu/ml in 5% dextrose. Size measurements of each sample were taken in 1 ml total volume in disposable cuvettes (Sartorius Stedim, Epsom, UK). Zeta potential measurements were taken in 1 ml total volume in disposable zetasizer cuvettes (Malvern Instruments). Default instrument settings and automatic analysis were used for all measurements.

Artificially enveloped Ad imaging by atomic force microscopy (AFM)

Twenty μl of a suspension containing 10^{11} Ad particles/ml was deposited on the surface of freshly cleaved mica (Agar Scientific, Essex, UK), and viruses were allowed to adsorb for 15 min. Unbound viruses were removed by washing with filtered dH_2O. Samples were then dried under a nitrogen stream. Imaging was carried out in TappingMode using a

Multimode AFM, E-type scanner, Nanoscope IV controller, Nanoscope 5.12b control software (all from Veeco, Cambridge, UK), and a silicon tapping tip (NSG01, NTI-Europe, Apeldoorn, The Netherlands) of 10 nm curvature radius, mounted on a tapping-mode silicon cantilever with a typical resonant frequency of 150 kHz and a force constant of 5.5 N/m, to image 5×5 μm square areas of the mica surface with a resolution of 512×512 pixels and a scan rate of 1 Hz. All AFM images were performed in air.

Determination of enveloped Ad biodistribution using radiotracers

Radiolabeling of the Ad capsid was conducted using a procedure similar to a previously described method (37). ^{125}I (200 μCi; GE Healthcare, Little Chalfont, UK) was diluted in 200 μl phosphate buffered saline (PBS), pH 7.4 (Invitrogen, Paisley, UK). Next, one Iodobead (Perbio Science, Cramlington, UK) was washed in PBS then blotted on Whatman paper and added to the ^{125}I stock. This was incubated at room temperature for 5 min. Ad.Null stock (200 μl containing 1×10^{12} pu) was diluted in 600 μl of PBS, and added to the tube containing the Iodobead and ^{125}I. The labeling reaction was allowed to proceed for 15 min at room temperature. To stop the reaction, the liquid sample was separated from the Iodobead and placed on ice. A Sepharose 4B column (GE Healthcare) was prepared by passing 1 ml of washing buffer (PBS containing 10% glycerol and 50 mM HEPES, pH 7.8; Sigma-Aldrich) through the column 3 times. The ^{125}I-labeled Ad (1 ml) was added to the column to remove any unincorporated ^{125}I. An additional 1 ml of washing buffer was added to the column, and the eluate was collected and disposed. Next, washing buffer was added in 500 μl portions, and 25 fractions of eluate were collected. Each fraction was placed on ice immediately after collection. Ten microliters of each fraction was added to a scintillation vial containing 1 ml of isopropanol and topped with 10 ml of Ready Organic scintillation cocktail (Beckman Coulter, High Wycombe, UK). Samples were placed in an LS6500 liquid scintillation counter (Beckman Coulter) and analyzed using the instrument's preset for ^{125}I.

Ad content of each fraction was determined using the PicoGreen assay (Invitrogen). Forty-five microliters from each sample was removed, and 5 μl of 0.5% sodium dodecyl sulfate (Sigma-Aldrich) was added to lyse the viral capsid. The lysed sample (20 μl) was added to duplicate wells of a black 96-well microplate (Greiner Bio-One, Stonehouse, UK). In addition, standards containing 10^8-10^{12} pu/ml of Ad were prepared as above. The PicoGreen reaction mix was prepared according to the manufacturer's protocol, and 180 μl was added to each well. Samples were incubated at room temperature for 5 min, and then read on a Wallac Viktor2 microplate reader (Perkin-Elmer, Beaconsfield, UK). Fractions 4–8, which contained the highest concentration of Ad, had a total of $\sim7 \times 10^{11}$ pu in 2.5 ml of washing buffer, as determined by fitting the PicoGreen results to the standard curve. These fractions were placed on a Vivaspin 4 centrifuge column [5000 molecular weight cutoff (mwco); Sartorius Stedim] and the sample was concentrated to a final volume of 700 μl (1×10^{12} pu/ml), placed in 50 μl aliquots, and frozen at −80°C prior to use for the biodistribution study.

Female BALB/c mice, 8–10 wk old, were purchased from Harlan UK (Blackthorn, UK) and housed under specific pathogen-free conditions for 1 wk after arrival to allow mice to acclimatize. Three mice per group were weighed, then anesthetized by intraperitoneal administration of a fentanyl-fluanisone (1–40 mg/kg) and midazolamine (20 mg/kg) mixture (Hypnorm/Hypnovel, Vet-Tech Solutions, Congleton, UK). Mice were warmed for 15 min in a heating box set at 37°C and were given 1×10^{10} pu of ^{125}I-labeled Ad alone, or enveloped in DMPC:Chol (2:1), DOTAP:Chol (2:1), or DOTAP:DOPE:DSPE-PEG$_{2000}$ (1:8:1), prepared as described above at a 3 mM total lipid concentration, in 200 μl of D5W by tail vein injection. Blood (100 μl) was collected from the tail vein by venipuncture 2 min, 5 min, 10 min, and 30 min postinjection. Mice were then killed by cervical dislocation. The right femoral artery was cut, and 10 ml of normal saline was injected through the heart to wash out the blood. The liver, spleen, right kidney, heart, lungs, and right femur were removed and weighed. In addition, a 100 mg piece of skin was shaved and excised from the back, and 100 mg of muscle was removed from the right thigh. The entire heart, spleen, kidney, lungs, and femur (following grinding using a mortar and pestle), and 100 mg pieces of the liver, skin, and muscle, or 100 μl of blood, were added to a 20 ml scintillation vial and topped with 1 ml of HTS-450 (both from Beckman Coulter), then placed in a 50°C shaking water bath overnight to dissolve the tissue. Samples were decolorized with 30% hydrogen peroxide (Sigma-Aldrich), and 70 μl of glacial acetic acid (Fisher Scientific, Loughborough, UK) was added to reduce chemiluminescence. Ten milliliters of Ready Organic scintillation cocktail was added, and samples were placed in LS6500 liquid scintillation counter (both from Beckman Coulter). Counts per minute data were analyzed using the instrument's preset for ^{125}I, including proprietary correction for chemiluminescence (Lumex) and color quenching (H-number plus).

Determination of enveloped Ad blood circulation time by real time quantitative polymerase chain reaction (PCR)

Female BALB/c mice, 6–10 wk old, were purchased from Harlan UK and housed as described above. Mice were warmed for 15 min in a heating box set at 37°C and anesthetized by isofluorane inhalation. At least 4 mice per group were injected i.v. *via* the tail vein with 1×10^{10} pu Ad.Null, 5×10^{10} pu Ad.Null, 1×10^{10} pu of DOTAP:DOPE:DSPE-PEG$_{2000}$-enveloped Ad.Null, or 5×10^{10} pu of DOTAP:DOPE:DSPE-PEG$_{2000}$-enveloped Ad.Null. For the low dose, 1 ml of enveloped Ad was prepared in 3 mM total lipid as described previously, and 200 μl of vector was administered. For the high dose of vector, 5 separate lipid films of each formulation were prepared and hydrated with Ad as described previously. After the 3 h stabilization period, the suspensions were combined and placed in the upper chamber of a Vivaspin 15, 5000 mwco centrifuge column (Sartorius Stedim), and were concentrated 5-fold to a 1 ml volume of D5W; 200 μl from this suspension was then administered. Blood was drawn from the tail vein by venipuncture, and 100 μl was collected in heparinized capillary tubes (Fisher Scientific) at 1 min, 10 min, 30 min, 4 h, and 48 h after vector administration. DNA was extracted from the blood using the QiaAmp DNA Micro Kit (Qiagen, Valencia, CA, USA) and following the manufacturer's instructions. Samples were eluted in 25 μl of buffer AE (10 mM Tris-Cl and 0.5 mM EDTA, pH 9.0), provided with the kit, and were stored at −20°C. Mice were maintained for an additional 30 days for determination of serum anti-Ad neutralizing antibody titer, as described below.

Prior to running PCR experiments, a set of 9 standards was created in duplicate containing viral DNA extracted, as described above, from 100 μl of mouse blood spiked with increasing amounts of Ad.Null particles (in 5-fold intervals from 1.28×10^5 to 5×10^{10} particles). The standards were run in parallel to all samples, and Ad particle numbers were

determined by fitting the threshold cycle from each unknown to the standard curve. Primers for the Ad fiber (5′-3′: TGG CTG TTA AAG GCA GTT TGG and GCA CTC CAT TTT CGT CAA ATC TT) have been described elsewhere (37) and were custom synthesized by Invitrogen. The Quantitect SYBR Green Kit (Qiagen), was used for the PCR reaction mix, and all samples were prepared in 96-well optical plates and sealed using Microseal B optical sealing film (both from Bio-Rad, Hemel Hempstead, UK). Reaction volume was 25 μl per sample, and primers were used at 200 nM concentrations. Two microliters of each sample or standard were added to the reaction mix, which was prepared according to the manufacturer's protocol. Samples were run on a Bio-Rad iQ3 Real-Time PCR Detection System using the following protocol: activation 95°C, 15 min, 1 cycle; denaturing, 95°C, 30 s; annealing, 60°C, 1 min; elongation, 72°C, 2 min (repeat last 3 for 40 cycles); this was followed by a melt curve analysis to verify PCR product specificity.

Assessment of neutralizing antibody titer

Mice injected with Ad.Null or DOTAP:DOPE:DSPE-PEG_{2000} for the quantitative PCR study described above were killed 30 days after vector administration, and whole blood was drawn from the inferior vena cava and placed on ice. Blood was also drawn from untreated mice. Samples were allowed to clot for 30 min, and then placed in a microcentrifuge at 8000 rpm for 10 min. The serum was separated and pooled for each group, then stored at −80°C until ready for use. Next, A549 cells (ATCC, Manassas, VA, USA) were grown to 70% confluence in 24-well tissue culture plates (VWR) in Dulbecco modified Eagle medium (DMEM) supplemented with 10% FBS and 1% penicillin/streptomycin (complete media), all from Invitrogen. Pooled serum was diluted 1:10 or 1:100 in 2 ml of DMEM containing 5×10^9 pu/ml of Ad.βgal, and all samples were incubated at 37°C for 30 min. Each sample (500 μl containing 1.25×10^9 pu of Ad.βgal) or of an equivalent dose of Ad.βgal incubated without any mouse serum was then added to triplicate wells of A549 cells and incubated for 90 min at 37°C. Cells were then washed in PBS, and incubated in complete media for 48 h. Cells were again washed in PBS and 200 μl of lysis buffer from the Tropix Galactolight Plus Kit (Applied Biosystems, Inc., Foster City, CA, USA) was added to each well. Plates were placed on a rocker for 10 min at room temperature and cell lysates were collected and centrifuged at 13,000 *g* to remove any debris, and 10 μl of the supernatant was analyzed for beta-galactosidase (β-gal) activity using the Tropix Galactolight Plus kit and a Berthold Lumat 9507 luminometer (Berthold Technologies, Redbourn, UK). Transgene expression in all wells was normalized to total albumin content using the Pierce BCA Assay Kit (Perbio Science).

In vivo gene transfer studies

Female BALB/c mice, 6–8 wk old, were purchased from Harlan UK and housed as described above. To prepare the vectors, DMPC:Chol, at a 2:1 M ratio, DOTAP:Chol, at a 2:1 M ratio, lipid films were formed and hydrated with a dispersion of 5×10^{10} pu of Ad.βgal in 1 ml of D5W, to yield a 3 mM final total lipid concentration (2 mM DMPC or DOTAP and 1 mM Chol). Mice were warmed to 37°C in a heating chamber, anesthetized using isofluorane, and administered Ad.βgal alone or enveloped in DMPC:Chol or DOTAP:Chol, in a 200 μl volume (a dose of 1×10^{10} pu/mouse) by tail vein injection. The mice were killed 48 h later, and tissue samples were harvested from the lung, liver (single lobe), spleen, and heart. Tissues were frozen immediately and stored at −80°C, then later thawed and homogenized using a Polytron homogenizer (Kinematica, Littau-Lucerne, Switzerland) in Tropix Galactolight Plus lysis buffer, 3 ml volume for liver and 2 ml for other tissues. The lysate was centrifuged at 13,000 *g* to removed any debris, and 10 μl of the supernatant was analyzed for β-gal activity as described above. All data was normalized for total albumin content using the Pierce BCA Protein Assay kit. In a separate experiment, an equivalent dose of empty DMPC:Chol or DOTAP:Chol liposomes prepared as above but without any Ad, was injected into mice as described. After 5 min, 1×10^{10} pu of Ad.βgal also was injected into the tail vein. After 24 h, mice were killed and tissue samples from the lung, liver, spleen, and heart were harvested and analyzed as described above.

In vivo tumor targeting studies

CT26 colon carcinoma cells (ATCC), syngeneic to BALB/c mice, were grown to log phase in Corning T75 flasks (Fisher Scientific). Cells were trypsonized and washed 3 times in PBS, then resuspended in PBS at a concentration of 1×10^7 cells per ml. Tumor cells (1×10^6 cells in 100 μl of PBS) were injected subcutaneously into each flank of 20 female BALB/c mice, 8–10 wk old, purchased from Harlan UK. Tumors were allowed to grow to 50–100 mm^2 (25 to 30 days after implantation), as determined by the product of the 2 largest perpendicular diameters. Mice were warmed for 15 min in a heating box set at 37°C and anesthetized by isofluorane inhalation. At least 4 mice per group were injected i.v. *via* the tail vein with Ad.βgal alone (2×10^{11} pu), DOTAP:DOPE:DSPE-PEG_{2000} (1:8:1) enveloped Ad.βgal, or DMPC:Chol:DSPE-PEG_{2000} (2:1:0.1) enveloped Ad.βgal. The remaining 3 mice were used as untreated controls. The DOTAP:DOPE:DSPE-PEG_{2000} envelope was prepared by adding 1 ml of a 5×10^{11} pu/ml dispersion of Ad.βgal in D5W to a dried lipid film as described previously to yield a 9 mM total lipid suspension. The DMPC:Chol:DSPE-PEG_{2000} envelope was prepared similarly to produce a 6.2 mM total lipid suspension. Duplicate films were prepared for each envelope, and the suspensions were combined prior to injection in a 400 μl volume. All animals were killed 3 days later, and the lung, liver (100 mg slice), spleen, and both flank tumors were excised and frozen at −80°C. Immediately prior to analysis, all samples were thawed and homogenized using a Polytron homogenizer in Tropix Galactolight Plus lysis buffer, 3 ml volume for liver, and 2 ml for all other tissues. The lysate then was centrifuged at 13,000 *g* to remove any debris, and 10 μl of the supernatant was analyzed for β-gal activity as described above.

RESULTS

Engineering artificially enveloped Ad suitable for extended blood circulation

We examined the effect of different lipid envelopes on Ad physicochemical properties. Ad (5×10^{10} pu) in distilled water containing 5% dextrose was added to a neutral (DMPC:Chol), cationic (DOTAP:Chol), or 2 PEG-lipid containing (DOTAP:DOPE:DSPE-PEG_{2000} and DMPC:Chol:DSPE-PEG_{2000}) lipid films to yield a 3 mM total lipid concentration. After bath sonication, the

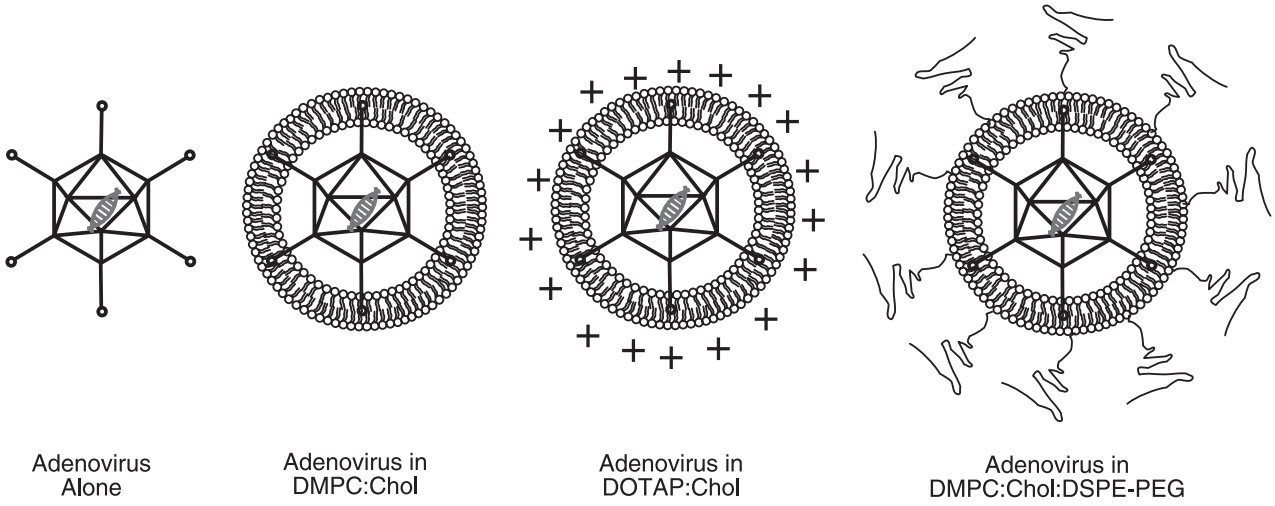

Figure 1. Schematic representation of artificially enveloped Ad engineered in this study.

hydrodynamic diameter and zeta potential (ζ) of the resulting vector suspensions were assessed by dynamic light scattering (DLS). **Figure 1** depicts schematics of the enveloped Ad vectors and **Table 1** summarizes the data from triplicate preparations of each type of enveloped vector.

To achieve passive tumor targeting, it is important that the vector is less than 200 nm in diameter to allow for long blood circulation times (38) and extravasation through the tumor fenestrated vasculature (39, 40). All 4 types of artificially enveloped Ad prepared (as shown in Table 1) were within the size range that would allow further *in vivo* investigation. The high polydispersity of the DMPC:Chol formulation is due to the lack of steric or electrostatic repulsion forces between the nanoparticles to prevent flocculation of the sample (*i.e.*, reversible sedimentation of the enveloped virions) during the 3 h stabilization period prior to the DLS measurement. The smaller size of the cationic enveloped virus systems was indicative of much stronger surface association between the viral surface and the envelope, leading to tighter wrapping around the anionic Ad capsid, as also confirmed by previous studies (36). However, such observations warrant further structural and biophysical studies to identify the conformational or structural changes of Ad surface proteins, such as the fibers, in the presence of the artificial lipid bilayer envelope. The ζ potential of the enveloped vector is determined by the type of lipids used: slightly negative for cholesterol containing zwitterionic envelopes and increasing from +22 to +60 mV as the DOTAP content increases from 10 mol % in the PEG-lipid envelope to 66 mol % for the DOTAP:Chol envelope. To obtain further structural information about the artificially enveloped Ad, samples were examined in air by AFM using the tapping mode (**Fig. 2**). The hydrated Ad and enveloped Ad samples were allowed to dry on a mica surface, and direct evidence of the lipid envelope around the Ad was observed (Fig. 2*b*, *c*).

In agreement with the DLS data, AFM imaging indicated that the cationic DOTAP:Chol envelope consisted of more tightly packed, multiple lipid bilayers (Fig. 2*b*), while the DMPC:Chol:DSPE-PEG$_{2000}$-enveloped Ad formed larger overall structures of fewer lipid bilayers wrapped around the virion (Table 1). The structural information using AFM reported here also agreed with prior electron microscopy studies (36). Combined, these data indicate that simply by altering the lipid composition of the envelope, artificially enveloped viruses can be engineered by self-assembly to possess custom-designed surface and structural properties.

TABLE 1. *Physicochemical characterization of artificially enveloped Ad*

Ad alone			Ad in DMPC:Chol			Ad in DOTAP:Chol			Ad in DOTAP:DOPE: DSPE-PEG			Ad in DMPC:Chol:DSPE-PEG		
Size (nm)	PI	ζ (mV)	Size (nm)	PI	ζ (mV)	Size (nm)	PI	ζ (mV)	Size (nm)	PI	ζ (mV)	Size (nm)	PI	ζ (mV)
117	0.08	–29	190	0.50	–5	65.6	0.21	+60	89	0.26	+23	134	0.31	–12
118	0.1	–30	224	0.45	–8	91.1	0.21	+62	88	0.27	+29	150	0.34	–13
118	0.07	–30	172	0.40	–5	71.2	0.26	+66	101	0.26	+22	136	0.30	–15

Three independent artificially enveloped Ad preparations are noted. Size is the hydrodynamic diameter; polydispersity index (PI) indicates size distribution of the enveloped adenovirus population; zeta potential (ζ) indicates average surface charge.

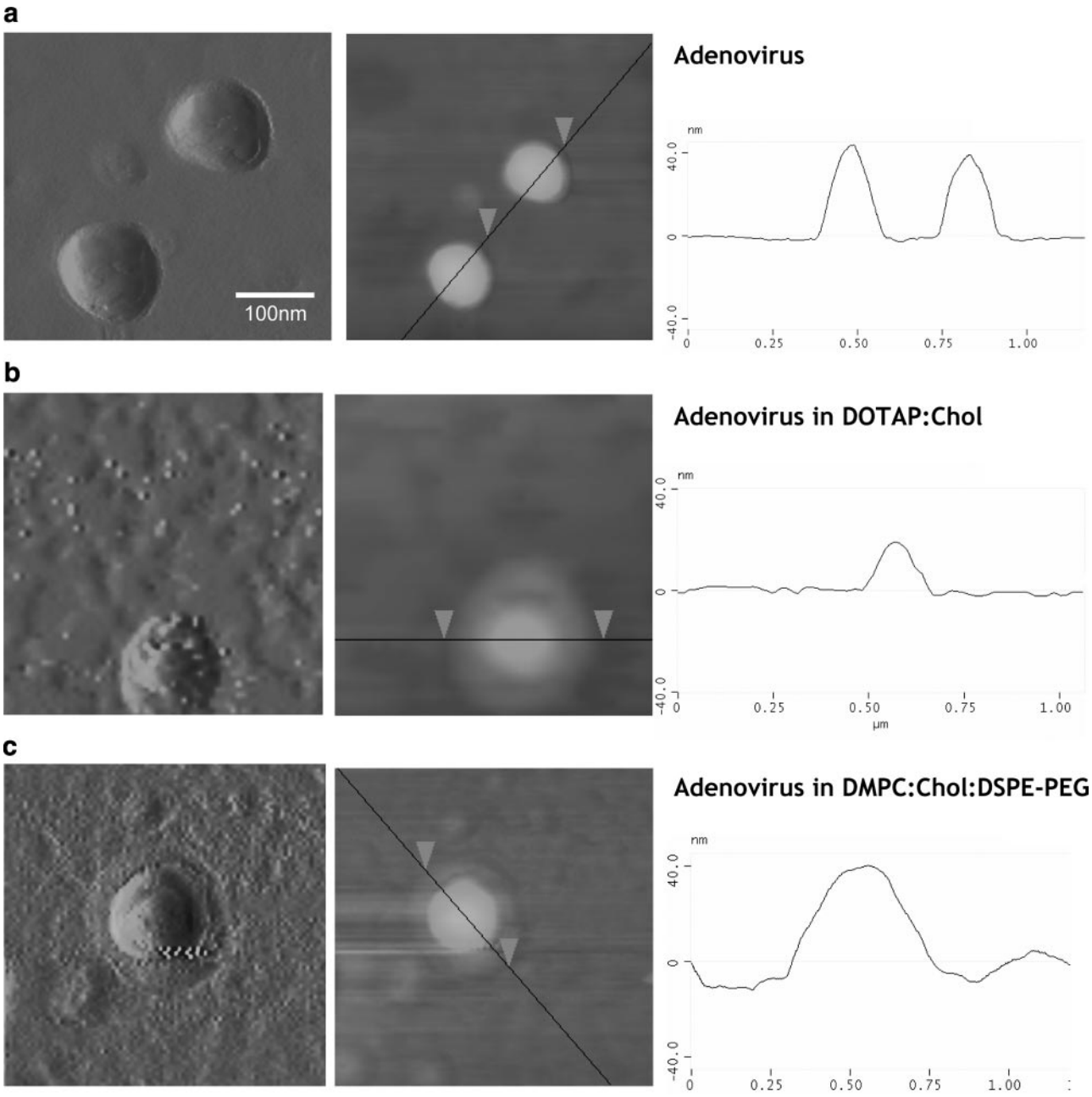

Figure 2. AFM of enveloped Ad. Samples (20 μl; 1×10^{11} Ad particles/ml) were deposited on mica and allowed to dry. The images for each of the following samples, scanning from left to right, are the amplitude image, the height image, and the cross-section analysis through the height image for Ad alone (*a*); DOTAP:Chol-enveloped Ad (*b*); and DMPC:Chol:DSPE-PEG_{2000}-enveloped Ad (*c*).

Artificially enveloped Ad exhibits prolonged blood circulation half-life

The effect of different envelopes on Ad biodistribution and blood clearance was assessed. The Ad capsid was radiolabeled with ^{125}I, and free iodine was separated by size exclusion chromatography. Like previous studies using similar techniques (37), our results show that ^{125}I-labeled Ad (quantified by the Picogreen assay) eluted in the column's void volume and was well separated from the unbound label (Supplemental Fig. 1). The radiolabeled virus alone (1×10^{10} pu), in a neutral (DMPC:Chol) envelope, a cationic (DOTAP:Chol) envelope, or a cationic, PEG-lipid (DOTAP:DOPE:DSPE-PEG_{2000}) envelope, was injected i.v. *via* the tail vein into BALB/c mice. Blood was drawn from the tail vein 2, 5, 10, and 30 min postinjection, and animals were killed at 30 min or 24 h postinjection for tissue biodistribution analysis.

The tissue affinity profiles of the lipid-enveloped Ad all showed significant uptake by the liver and spleen 30 min following administration (**Fig. 3**), indicating that

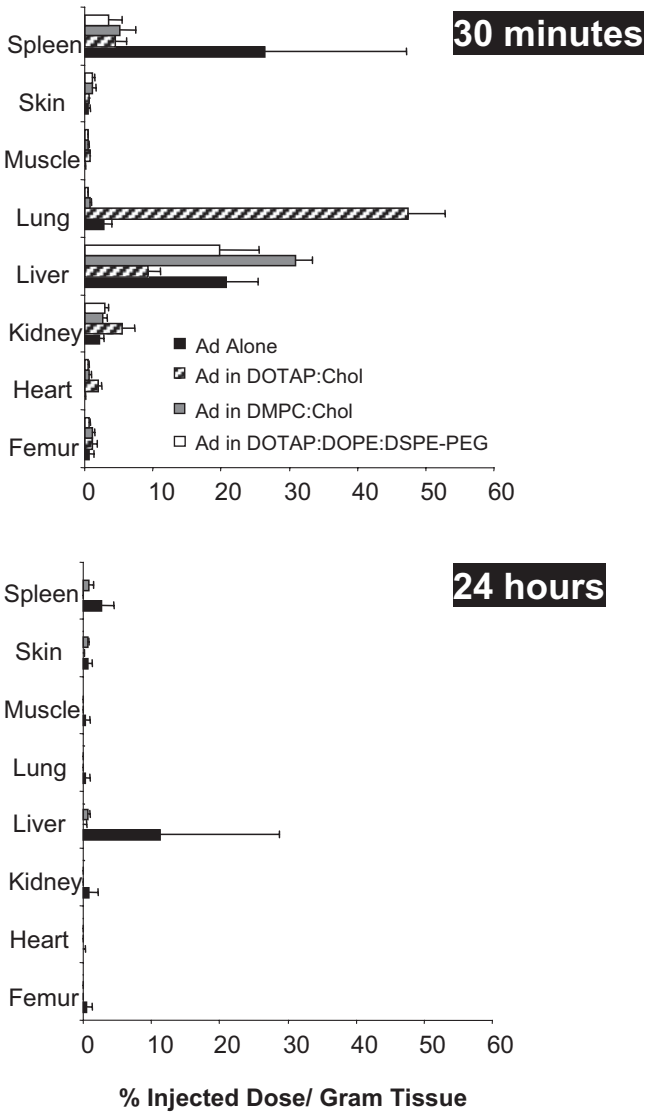

Figure 3. Determination of enveloped Ad biodistribution using radiotracers. Mice were injected i.v. with 1×10^{10} pu of naked ^{125}I-Ad, or ^{125}I-Ad in DMPC:Chol (2:1), DOTAP:Chol (2:1), or DOTAP:DOPE:DSPE-PEG2000 (1:8:1) *via* the tail vein. The listed organs were weighed and analyzed for ^{125}I content 30 min or 24 h later. Data are expressed as the percentage of the radioactivity in the total dose injected (determined by measurement of the radioactivity of 1×10^{10} pu of ^{125}I-Ad at the time of analysis) per gram of tissue + SD. At least 3 mice per group were used.

the majority of enveloped and nonenveloped Ad were cleared by tissue macrophages. Strikingly, the DOTAP:Chol-enveloped vector showed a high degree of affinity for the lung, nearly 47% of the injected dose (i.d.) per gram of tissue. By comparison, only 2.7% i.d./g tissue was found in the lungs of mice administered naked Ad. Uptake of the cationic, PEG-lipid enveloped vector was reduced in the liver, spleen, and lung as compared to Ad, while uptake of the DMPC:Chol-enveloped Ad was slightly increased in the liver, but reduced in the spleen and lung.

Neutral liposomes of similar size to the ones studied in this report have been shown to enhance the blood circulation half-life of encapsulated small molecules, though significant uptake by the liver with lower levels of splenic uptake were observed (41). The use of sterically stabilized liposomes prolonged blood circulation time due to reduced interactions with the mononuclear phagocyte system (MPS), and it has been shown that inclusion of both short and long chain PEG-lipids can extend the blood circulation time of cationic liposomes (42). Therefore, our observations were consistent with the hypothesis that lipid-enveloped Ad will behave like a liposome of the equivalent physicochemical characteristics.

Our data for the blood clearance profile of ^{125}I-labeled naked Ad (**Fig. 4*a***) recapitulated a previously published report that ~10% of the injected dose of radioactivity remained in circulation 30 min after i.v. administration of Ad (37). This level is believed to be due to radiolabeled capsid fragments or viral degradation products, with less than 1% representing intact viral capsids. Plasma levels of artificially enveloped Ad were found to be significantly increased using the PEG-lipid envelope 10 and 30 min postinjection compared to naked Ad. DOTAP:Chol-enveloped Ad appeared to be more rapidly cleared from the blood, while there was little difference in the clearance profiles between the zwitterionic (DMPC:Chol) enveloped Ad and Ad alone.

Because of the high level of background radioactivity in the blood due to capsid fragments, the radiotracer studies were used only as a means of screening different envelopes for extended blood circulation time. As viral degradation occurs after the vector exits the blood and is taken up by the cells of a particular organ, any degradation product remaining within the tissue still represents virus that was internalized by that tissue, and therefore direct measurement of radiolabeled Ad within an organ is an accurate measure of tissue biodistribution. However, these degradation products are later returned to the bloodstream; thus, portions of the same viral particles may be detected in the blood more than once, leading to the observed increase in background radioactivity. To identify intact virions in the blood, a quantitative PCR protocol was used. The radiolabeling studies indicated that Ad in a PEG-lipid envelope was cleared from the bloodstream more slowly than nonenveloped Ad. Because the dose of Ad administered to the systemic circulation will affect the blood clearance rate (43), we compared the blood circulation time of 1×10^{10} pu or 5×10^{10} pu of Ad alone or in the DOTAP:DOPE:DSPE-PEG$_{2000}$ envelope. In Fig. 4*b*, we observed that at both doses, when compared to Ad alone, almost 10-fold more enveloped Ad was found in the bloodstream for up to 48 h after vector administration. This result is consistent with other studies in which the blood clearance rate of polymer-conjugated Ad was compared to Ad alone (37).

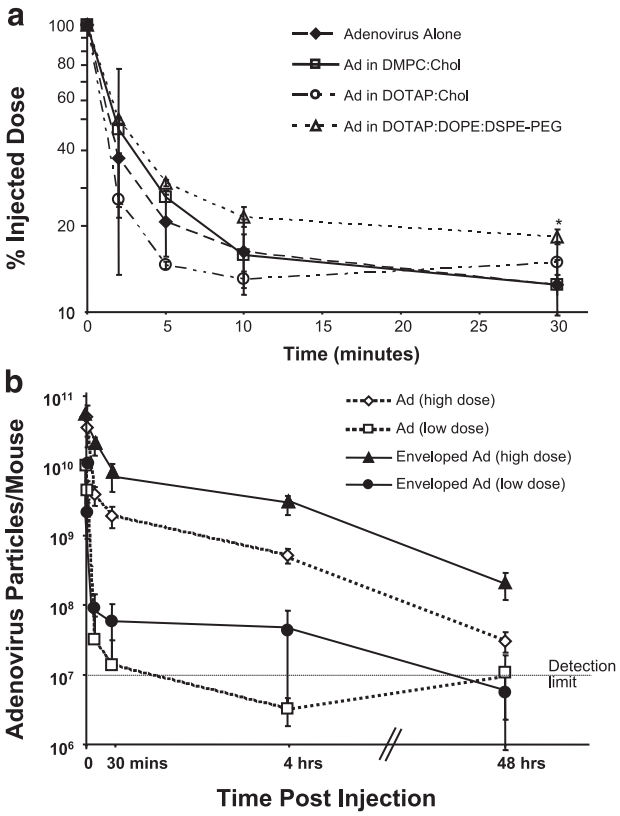

Figure 4. Assessment of enveloped Ad blood circulation time. *a*) Ad was radiolabeled with ^{125}I, and 1×10^{10} pu of naked ^{125}I-Ad, ^{125}I-Ad in DMPC:Chol, DOTAP:Chol, or DOTAP:DOPE:DSPE-PEG$_{2000}$ envelopes was injected i.v. Blood was drawn from the tail vein over 30 min, and radioactivity was calculated as a percentage of the injected dose. *b*) Mice were injected i.v. with 1×10^{10} pu of naked Ad and DOTAP:DOPE:DSPE-PEG$_{2000}$-enveloped Ad (low dose), or 5×10^{10} pu of naked Ad and DOTAP:DOPE:DSPE-PEG$_{2000}$-enveloped Ad (high dose). Blood was drawn over 2 days, and the Ad content was determined by quantitative real time PCR. Data are expressed as the mean ± SD of at least 3 mice per group. *$P < 0.05$ *vs.* naked Ad.

Decreased antibody responses to artificially enveloped Ad

To be effective in a clinical setting, it is likely that enveloped Ad will need to be administered to a patient several times. However, repeat administration of adenoviral vectors is limited due to production of high levels of adenoviral-specific neutralizing antibodies by the host (44). Therefore, the neutralizing antibody response in mice was assessed 30 days following intravenous injection of Ad.Null alone (5×10^{10} pu) or DOTAP:DOPE:DSPE-PEG$_{2000}$-enveloped Ad.Null. Non-enveloped Ad.βgal was incubated with 10 or 100-fold dilutions of serum taken from these mice, and then was used to transfect cells. β-gal activity was assessed 24 h later with low level expression indicating inhibition of Ad infectivity due to the presence of neutralizing antibodies in the serum (**Fig. 5**). We found that the neutralizing antibody titer of mice administered with the enveloped Ad was ~3-fold less than that of mice injected with naked Ad. This data indicated that the lipid envelope can significantly reduce the immunogenicity of Ad and is particularly important in light of earlier studies which have shown that Ad capsid proteins mixed with preformed liposomes can enhance the immune response (45). More comprehensive immune response studies should be carried out to explore the extent of masking offered by the different artificial envelopes.

Artificial envelopment of Ad ablates gene transfer to liver and spleen *in vivo*

One of the major hurdles to delivering any type of Ad to diseased tissue *via* the systemic circulation is the reduction of native viral tropism, and more specifically gene transfer to the liver and spleen. Our *in vitro* studies indicated that binding to CAR was significantly disrupted following lipid envelopment of Ad (36). To investigate how an artificial envelope affected the Ad gene transfer biodistribution *in vivo*, a cationic DOTAP:Chol lipid bilayer and a zwitterionic DMPC:Chol bilayer were constructed around Ad.βgal and the resulting vectors were injected i.v. into mice. The gene transfer activity of the enveloped vectors was analyzed in the liver, spleen, lungs, and heart, the primary tissue targets for Ad vectors (8) (**Fig. 6*a***). For both types of envel-

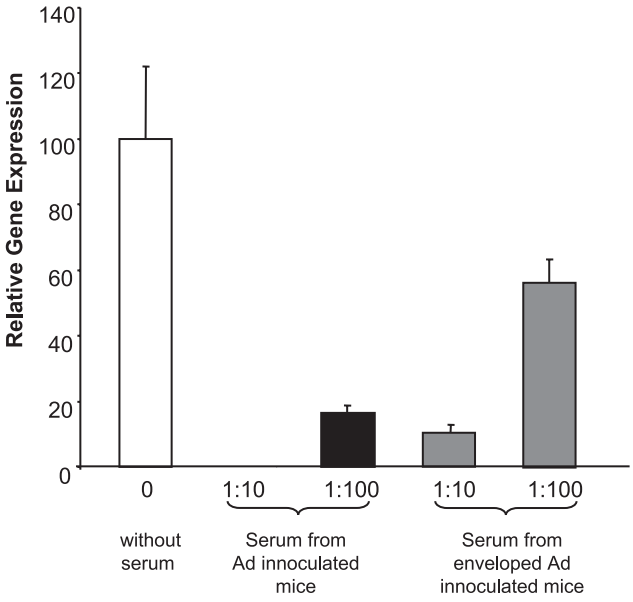

Figure 5. Assessment of neutralizing antibody titer in mice treated with naked or enveloped adenovirus. Mice were injected i.v. with 5×10^{10} pu of naked Ad or DOTAP:DOPE:DSPE-PEG$_{2000}$-enveloped Ad. Blood was drawn 30 days later, and serum was separated and pooled for each condition. Ad.βgal was incubated with dilutions of serum from the treated mice and added to triplicate wells of A549 cells. After 24 h, cells were analyzed for β-gal expression, and activity was normalized to total albumin content. Data are expressed as the percentage of the β-gal activity in cells treated with Ad in the absence of mouse serum (shown on the left) ± SE. For both dilutions of serum from DOTAP:DOPE:DSPE-PEG$_{2000}$-enveloped Ad injected mice, $P < 0.01$ *vs.* the equivalent dilution of serum from naked Ad injected mice.

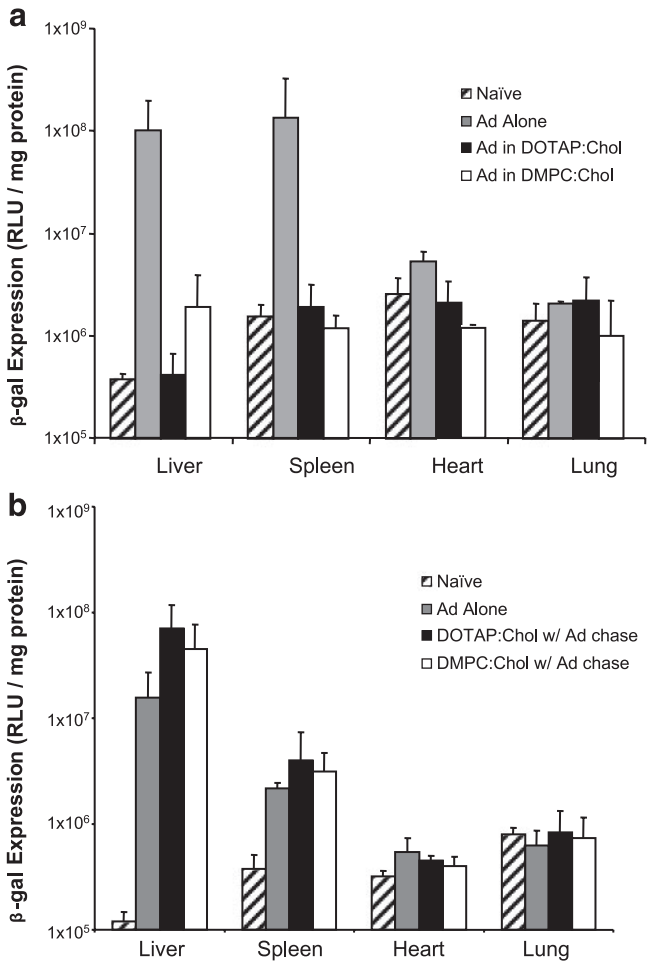

Figure 6. *In vivo* gene transfer of i.v. injected enveloped Ad.βgal. *a*) Mice were injected i.v. with 1×10^{10} pu of naked Ad, DMPC:Chol-enveloped Ad, or DOTAP:Chol-enveloped Ad. After 48 h, organs were assessed for β-gal expression. *b*) Mice were sequentially injected i.v. with empty DMPC:Chol or DOTAP:Chol liposomes, followed 5 min later by 1×10^{10} pu of naked Ad. After 48 h, organs were assessed for β-gal expression. Data are expressed as the mean ± SD of at least 3 mice per group.

oped Ad vectors, transgene expression was reduced more than 100-fold in the liver and spleen as compared to Ad alone. β-Gal expression in the lungs was found to be similar in mice administered either Ad alone or DOTAP:Chol-enveloped Ad, and was reduced to background levels for the DMPC:Chol-enveloped vector.

Figure 6*b* shows the *in vivo* gene transfer activity of Ad.βgal injected 5 min after an initial intravenous injection of either empty DOTAP:Chol or DMPC:Chol liposomes. When injected prior to administration of Ad, liposomes enhanced gene expression in the liver and spleen as compared to Ad administered in the absence of liposomes. This result confirmed that it was necessary to envelope the Ad capsid prior to intravenous injection in order to achieve the reduction in hepatic and splenic gene transfer that was observed in Fig. 6*a*. Overall, these experiments illustrated that artificial envelopment of Ad vectors led to dramatically reduced gene transfer to the liver and spleen. Combined with the extended blood circulation, reduced gene transfer to the liver and spleen is critical when targeting a cytotoxic transgene or for use of a prodrug strategy for treatment of cancer. Therefore, use of enveloped Ad should greatly reduce the toxicity of systemically delivered virus.

Artificial envelopment leads to preferential Ad gene transfer to solid tumors *in vivo*

To evaluate the tumor targeting and gene expression capability of artificially enveloped Ad, CT26 cells were implanted in the flanks of BALB/c mice and once tumors were established, Ad.βgal alone (2×10^{11} pu) and Ad.βgal. enveloped in DOTAP:DOPE:DSPE-PEG_{2000} or DMPC:Chol:DSPE-PEG_{2000} were injected *via* the tail vein. Mice were killed 3 days later, and the liver, spleen, lung, and tumors were analyzed for β-gal expression. The results of this experiment are shown in **Fig. 7**.

Neither Ad alone nor DOTAP:DOPE:DSPE-PEG_{2000}-enveloped Ad effectively transfected the tumors following systemic administration. However, DMPC:Chol:DSPE-PEG_{2000}-enveloped Ad appeared to transfect the tumor (P=0.05 *vs.* untreated mice) and, like DOTAP:DOPE:DSPE-PEG_{2000}-enveloped Ad, had nearly 100-fold less gene expression in the liver and spleen than naked Ad. This result indicated that it was possible to target enveloped Ad to tumors through the EPR effect, and at the same time reduce gene transfer to nontarget tissue. However, it is clear that effective delivery of enveloped Ad to treat tumors will require careful choice of envelope and vector dosing regimen. More

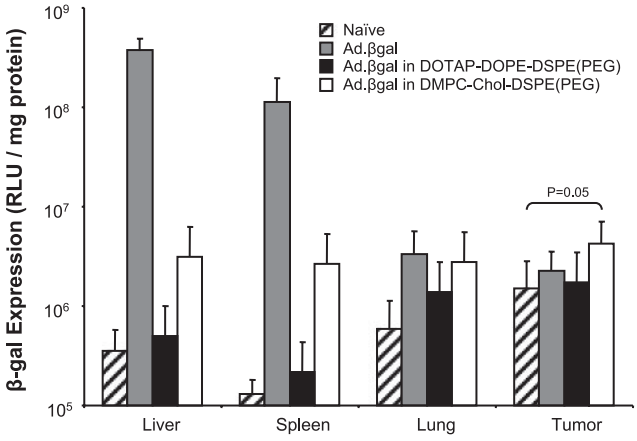

Figure 7. *In vivo* gene transfer of i.v. injected stealth enveloped Ad.βgal in tumor bearing mice. BALB/c mice bearing CT26 tumors on both flanks were treated with 2×10^{11} pu Ad.βgal alone, DOTAP:DOPE:DSPE-PEG_{2000}-enveloped Ad.βgal, or DMPC:Chol:DSPE-PEG_{2000}-enveloped Ad.βgal. After 3 days, organs plus tumors were analyzed for β-gal activity by chemiluminescence. Data are the mean + SD of at least 3 mice, expressed as β-gal activity (relative light units) normalized to total albumin content of each tissue.

research will be necessary using preclinical tumor treatment models to achieve tumor-specific transgene expression at therapeutic levels.

DISCUSSION

Ad is one of the most efficient gene delivery vehicles. Translocation from the cell surface to the nucleus is extremely rapid and far more efficient than nonviral gene delivery vectors (46). The capacity to carry a large genetic payload that can be modified to be highly tumor specific makes it very attractive for development as an anticancer medicine. However, numerous barriers to intravenous delivery of Ad must be overcome before it can truly be useful for cancer therapy. First, Ad must avoid clearance from the bloodstream and uptake by nontarget tissue. Unfortunately, Ad is rapidly cleared from circulation by the MPS (8), with a blood half-life in mice of less than 2 min (10), and readily infects the liver and spleen, leading to severe hepatotoxicity at high doses (47, 48). Second, Ad must overcome transvascular and extracellular barriers in order to pass through tumor microvessel fenestrae and diffuse through the extracellular matrix to even reach tumor cells. While the nanoscale of Ad virions allows them to pass through vessel pores, dissemination into solid tissue and tumors is limited to the needle tract following direct tissue administration of Ad (49, 50). Finally, even if Ad reaches a cancer cell, it must be efficiently internalized; however, Ad infectivity of tumors has been shown to be poor due to generally low levels of CAR expression by tumor cells (28). With these limitations in mind, an artificial envelopment strategy was developed to mask the Ad surface in order to block native tropism, extend blood residence time, and enhance tumor targeting. In addition, the envelopes were selected to enhance Ad penetration into tumors and maintain a particle size of less than 200 nm.

Liposomes have been shown to be very effective at delivering blood borne therapeutic agents to cancer cells. Features such as size (51) and surface charge (40) can easily be manipulated to enhance accumulation in tumors. Therefore, we hypothesized that a hybrid system, in which Ad was wrapped in a lipid envelope, would provide an ideal modular platform for the development of anticancer genetic medicines. The interaction of Ad with preformed liposomes has been described in numerous studies. Complexes of preformed, cationic liposomes and Ad have been shown to be effective at enhancing adenoviral gene transfer to tumor cells expressing low levels of CAR (52), and these complexes are resistant to inhibition by neutralizing antibodies (31). Injecting these vectors directly into solid tumors has been reported to lead to enhanced gene transfer and greater tumor retention than injection of naked Ad (52–54).

We recently described a method for reproducible and facile construction of artificial lipid envelopes for Ad (36). Prior to our work, others reported a different liposome-encapsulated Ad, generated by mixing preformed liposomes with the virus, which was resistant to Ad-specific neutralizing immunity both *in vitro* and *in vivo* (30). However, systems based on the mixing of oppositely charged nanoparticles such as the anionic Ad and cationic liposomes are inherently unstable and prone to aggregation (55), making characterization and systematic manipulation difficult and pharmacological use unreliable. This fact has led to conflicting reports regarding the occurrence of encapsulation and the structures formed following mixing of Ad with preformed cationic liposomes. Both Yotna *et al.* (30) and Meunier-Dumont *et al.* (56)reported that preformed cationic liposomes may encapsulate the Ad in multiple lipid layers. On the other hand, Qui *et al.* (27) observed that mixing Ad with preformed cationic liposomes produced virus-liposome aggregates without report of any encapsulation. Because dissemination into tumor vasculature requires that vectors be less than 200 nm in diameter (51), the ability to control vector size is a matter of critical importance. Further, the previously described liposome encapsulated vector systems are limited to cationic liposome formulations, and reduction in gene transfer to the liver and spleen has not been demonstrated. The artificial envelopment of Ad described in our study does not involve mixing virions with preformed cationic liposomes. Instead, it allows for the spontaneous self-assembly of the envelopes around the viral surface, and constitutes a general strategy to engineer viral surfaces to achieve specific pharmacological and biological goals.

Interest in encapsulating nanoparticles in liposomes to generate solid-core liposomes has increased in recent years (26, 57), and the feasibility of delivering solid nanoparticles to cells using fusogenic liposomes has been demonstrated (58). Herein it is shown that it is possible to encapsulate virions, which possess a far more complicated surface chemistry than the chitosan or polystyrene nanoparticles previously described. Artificial lipid envelopes for Ad could be created from zwitterionic, cationic, PEG-lipid, and cationic/PEG-lipid formulations. In all cases, vector size was reduced below 200 nm by bath sonication and surface charge characteristics were reproducible, thermodynamically stable and identical to liposome-alone systems.

Notably, when injected *in vivo*, the biodistribution and blood clearance profiles of lipid-enveloped Ad appeared consistent with the expected distribution of the equivalent liposome-alone systems. A neutral DMPC:Chol envelope, a strongly cationic DOTAP:Chol envelope, and a less positively charged, sterically stabilized envelope consisting of DOTAP:DOPE:DSPE-PEG_{2000} were formulated to wrap Ad and the resulting vectors were injected i.v. into mice. As reported for other types of neutral liposomes (41), DMPC:Chol-enveloped Ad was found in the liver and spleen, and it possessed very similar blood kinetics to naked Ad. Following envelopment in cationic DOTAP:Chol bilay-

ers, Ad blood clearance rate and the affinity for the lung both were increased. Krasnici *et al.* (59) observed that highly cationic liposomes can be effective in targeting tumor vasculature and are retained by the tumor for up to 6 h after injection. However, the total lipid dose used in our DOTAP:Chol-enveloped Ad study was less than 1/10th of that used by Krasnici *et al.* At this lower dose, the MPS may not be sufficiently overwhelmed, leading to faster blood clearance. The cationic, PEG-lipid envelope extended Ad blood circulation time and greatly reduced spleen affinity as compared to naked Ad, but because of the lower surface charge, there was no increase in lung affinity. These results are comparable to previously published reports regarding the biodistribution of similar liposome-alone formulations (40).

Note that increased accumulation of DOTAP:Chol-enveloped Ad in the lung did not lead to enhanced gene transfer in that tissue. It has previously been reported that shortly after intravenous injection of cationic lipoplexes (60) and other positively charged nanoparticles (61), high lung accumulation occurs, but only in a transient manner. Unless highly binding or capable of fusing with the membranes of the pulmonary vasculature, the majority of particles accumulating in the lung do not reside there long. Generally, at longer time points after i.v. injection of cationic nanoparticles, the number of particles in the lung decreases and a corresponding increase in particle number is observed in the liver and spleen, though this is size dependent. DOTAP:Chol-enveloped Ad likely follows the same transient pattern of tissue distribution, and therefore, no increase in gene transfer is observed in the lung.

Other researchers have reported that overwhelming the MPS with a high dose of Ad (43) or ablation of tissue macrophages using clondronate liposomes (62) can extend the blood circulation time of Ad. Interestingly, there are two conflicting reports relating to sequential administration of preformed liposomes followed by naked Ad. Snoeys *et al.* (63) reported that preinjection of egg yolk phosphatidylcholine liposomes enhanced gene transfer to the liver, similar to our findings with empty DMPC:Chol liposomes and Ad. Ma *et al.* (32) reported that preinjection of DOTAP liposomes followed by Ad led to an increase in gene transfer to the lungs and a relative decrease in gene transfer to the liver. However, we observed increased gene expression in the liver, spleen, and lungs of animals sequentially injected with DOTAP:Chol liposomes followed by 1×10^{10} pu of naked Ad. It is possible that the different outcomes arise from differences in the experimental design between our study and that of Ma *et al.* (32), including differences in lipid dose (0.9 μmol for Ma *et al. vs.* 0.6 μmol in our study), Ad dose (Ma *et al.* observed optimal lung targeting at a dose of 4×10^{10} pu), lipid molecules, and the timing between injections. As noted above, there were clear alterations in the blood clearance rates of Ad enveloped in three different lipid bilayer formulations. Although the dose of lipid and virus injected was identical for all three groups, the cationic envelope led to more rapid clearance of Ad from the bloodstream, which may indicate that this lipid/virus dose was not sufficient to overwhelm the MPS. Therefore, it is unlikely that overwhelming the MPS alone accounts for the increase in blood circulation time observed for DOTAP:DOPE:DSPE-PEG_{2000}-enveloped Ad.

Although high levels of gene expression and detectable levels of radiolabeled capsid remained in mice injected with naked Ad, our biodistribution and *in vivo* gene transfer data at 24 h postinjection indicated that the enveloped Ad capsid was cleared from all organs. In addition, little transgene expression was observed, even in the liver and spleen, the primary targets of naked Ad. Enveloped viruses may not bind efficiently to normal tissue and cells, such as hepatocytes, and likely are cleared from the circulation and liver sinusoids by macrophages. One of the unique properties of nanoscale liposomes and nanoparticles in general (<200 nm) is their ability to accumulate in vascularized tumors following extravasation from the central circulation by the EPR effect (64). This becomes even more pronounced when components that interfere with clearance by the MPS, such as PEG-lipid conjugates, are incorporated into liposomes, greatly decreasing their blood clearance rate (39, 65). Although Ad is a nanoparticle <100 nm in diameter, it does not benefit from the EPR effect due to a wide range of interactions between the viral capsid and host cells and proteins which lead to extremely rapid clearance from the bloodstream by the MPS. There have been many strategies to reduce the interaction of Ad with nontarget tissue and to extend blood residence time through modification of Ad genetic, chemical, or colloidal properties, and mixed results have been achieved (66).

Because it was possible to wrap Ad with a PEG-lipid bilayer to construct an artificially enveloped Ad vector less than 200 nm in diameter that exhibited an extended blood circulation time as compared to naked Ad, we believed that such enveloped Ad vectors might accumulate in well-vascularized solid tumors more efficiently than naked Ad. However, our initial pilot studies in tumor bearing mice i.v. injected with DOTAP:DOPE:DSPE-PEG_{2000}-enveloped Ad indicated that very little gene transfer occurred in any tissue, including the tumors (data not shown). Similar empty cationic liposomes have been shown to have a greater association with tumor vasculature and possibly less penetration into the tumor interstitium than neutral formulations (40). We hypothesized that lack of interstitial penetration might account for the absence of gene expression; therefore, we developed a DMPC:Chol:DSPE-PEG_{2000} envelope. Similar liposomal formulations are known to penetrate into the tumor perivascular space (67). When Ad was enveloped in this bilayer, tumor-specific gene transfer was found following i.v. administration. β-Gal expression in the tumors of mice injected with naked Ad was far more variable than in the DMPC:

Chol:DSPE-PEG_{2000} enveloped Ad treated mice, and was not statistically significant *vs.* naive animals ($P>0.1$). We hypothesize that the DMPC:Chol:DSPE-PEG_{2000} envelope may allow increased Ad tumor permeation and retention. However, Ad infectivity likely is reduced by lipid envelopment, leading to the low level of gene transfer observed. Following extravasation from the tumor vasculature, enveloped Ad may be trapped in the perivascular tumor regions where the lipid envelope gradually becomes unstable, leading to escape of naked Ad, which then transfects the tumor cells. Such mechanistic interpretations, though indirect and speculative, are supported by our recent demonstration that lipid enveloped Ad vectors could be designed to penetrated more deeply than Ad alone into a three-dimensional tumor spheroid (36). This has great implications for the development of the next generation of lipid enveloped Ad. It appears that it is necessary to enhance both tumor localization and penetration within the tumor interstitial space to achieve any degree of gene transfer.

The unique characteristics of tumor physiology that may allow for Ad escape from the lipid envelopes within tumor tissue need further investigation. Notably, the CT26 tumors used for this study have been reported to be CAR deficient (68), indicating that enveloped Ad can effectively deliver genes to tumors normally not infected by naked Ad. Prior to the present study, an Ad vector modified with a multivalent polymer covalently bound to capsid proteins also was shown to passively accumulate in, and transfect solid tumors in the absence of high liver and spleen gene transfer, following intravenous injection into mice (35). However, clinical development of this vector will be hampered by difficulties in production and purification, and further modulation of the vector characteristics will not be facile due to limited possibilities offered by conjugation chemistries. The envelopment process we have developed may eliminate these barriers to the generation of a long-circulating, tumor targeting adenoviral platform suitable for clinical use.

In conclusion, we were able to achieve tumor-specific targeting of Ad through rational design of the features of an artificial Ad envelope. We demonstrated that 4 different types of lipid enveloped adenoviral vectors, when prepared under the same controlled conditions, did not efficiently infect the liver and spleen—the two dose-limiting organs in adenoviral gene therapy. These enhancements are critical for improving the efficacy/toxicity ratio in viral gene therapy. In the future, further improvements in vector design may be possible through optimization of the lipid envelope to increase tumor penetration, and for use in other tissues (such as the brain and muscle) where dissemination is a problem. By combining lipid bilayer biophysics and self-assembly with the highly efficient intracellular trafficking and gene transfer of Ad, this study provides the basis for development of a novel vector platform for gene therapy or oncolytic virotherapy of cancer, and for systemic delivery of Ad to multiple, widespread, and disseminated targets. In a broader context, this work illustrates the capability to build artificial envelopes around nonenveloped virions by self-assembly, and the dramatic implications that such a strategy has on altering and modulating the *in vivo* biological function of viruses. FJ

REFERENCES

1. Alemany, R., Gomez-Manzano, C., Balague, C., Yung, W. K., Curiel, D. T., Kyritsis, A. P., and Fueyo, J. (1999) Gene therapy for gliomas: molecular targets, adenoviral vectors, and oncolytic adenoviruses. *Exp. Cell Res.* **252,** 1–12
2. Anklesaria, P. (2000) Gene therapy: a molecular approach to cancer treatment. *Curr. Opin. Mol. Ther.* **2,** 426–432
3. Bauerschmitz, G. J., Barker, S. D., and Hemminki, A. (2002) Adenoviral gene therapy for cancer: from vectors to targeted and replication competent agents (review). *Int. J. Oncol.* **21,** 1161–1174
4. Fang, B., and Roth, J. A. (2003) The role of gene therapy in combined modality treatment strategies for cancer. *Curr. Opin. Mol. Ther.* **5,** 475–482
5. Gomez-Navarro, J., and Curiel, D. T. (2000) Conditionally replicative adenoviral vectors for cancer gene therapy. *Lancet Oncol.* **1,** 148–158
6. Morral, N., O'Neal, W. K., Rice, K., Leland, M. M., Piedra, P. A., Aguilar-Cordova, E., Carey, K. D., Beaudet, A. L., and Langston, C. (2002) Lethal toxicity, severe endothelial injury, and a threshold effect with high doses of an adenoviral vector in baboons. *Hum. Gene Ther.* **13,** 143–154
7. Rivera, A. A., Davydova, J., Schierer, S., Wang, M., Krasnykh, V., Yamamoto, M., Curiel, D. T., and Nettelbeck, D. M. (2004) Combining high selectivity of replication with fiber chimerism for effective adenoviral oncolysis of CAR-negative melanoma cells. *Gene Ther.* **11,** 1694–1702
8. Worgall, S., Wolff, G., Falck-Pedersen, E., and Crystal, R. G. (1997) Innate immune mechanisms dominate elimination of adenoviral vectors following *in vivo* administration. *Hum. Gene Ther.* **8,** 37–44
9. Worgall, S., Leopold, P. L., Wolff, G., Ferris, B., Van Roijen, N., and Crystal, R. G. (1997) Role of alveolar macrophages in rapid elimination of adenovirus vectors administered to the epithelial surface of the respiratory tract. *Hum. Gene Ther.* **8,** 1675–1684
10. Alemany, R., Suzuki, K., and Curiel, D. T. (2000) Blood clearance rates of adenovirus type 5 in mice. *J. Gen. Virol.* **81,** 2605–2609
11. Kanerva, A., and Hemminki, A. (2004) Modified adenoviruses for cancer gene therapy. *Int. J. Cancer* **110,** 475–480
12. Martin, K., Brie, A., Saulnier, P., Perricaudet, M., Yeh, P., and Vigne, E. (2003) Simultaneous CAR- and αV integrin-binding ablation fails to reduce Ad5 liver tropism. *Mol. Ther.* **8,** 485–494
13. Wu, H., Seki, T., Dmitriev, I., Uil, T., Kashentseva, E., Han, T., and Curiel, D. T. (2002) Double modification of adenovirus fiber with RGD and polylysine motifs improves coxsackievirus-adenovirus receptor-independent gene transfer efficiency. *Hum. Gene Ther.* **13,** 1647–1653
14. Douglas, J. T., Rogers, B. E., Rosenfeld, M. E., Michael, S. I., Feng, M., and Curiel, D. T. (1996) Targeted gene delivery by tropism-modified adenoviral vectors. *Nat. Biotechnol.* **14,** 1574–1578
15. Kim, J., Smith, T., Idamakanti, N., Mulgrew, K., Kaloss, M., Kylefjord, H., Ryan, P. C., Kaleko, M., and Stevenson, S. C. (2002) Targeting adenoviral vectors by using the extracellular domain of the coxsackie-adenovirus receptor: improved potency via trimerization. *J. Virol.* **76,** 1892–1903
16. Brandao, J. G., Scheper, R. J., Lougheed, S. M., Curiel, D. T., Tillman, B. W., Gerritsen, W. R., van den Eertwegh, A. J., Pinedo, H. M., Haisma, H. J., and de Gruijl, T. D. (2003) CD40-targeted adenoviral gene transfer to dendritic cells

through the use of a novel bispecific single-chain Fv antibody enhances cytotoxic T cell activation. *Vaccine* **21,** 2268–2272
17. Fisher, K. D., Stallwood, Y., Green, N. K., Ulbrich, K., Mautner, V., and Seymour, L. W. (2001) Polymer-coated adenovirus permits efficient retargeting and evades neutralising antibodies. *Gene Ther.* **8,** 341–348
18. Pearce, O. M., Fisher, K. D., Humphries, J., Seymour, L. W., Smith, A., and Davis, B. G. (2005) Glycoviruses: chemical glycosylation retargets adenoviral gene transfer. *Angew. Chem. Int. Ed. Engl.* **44,** 1057–1061
19. O'Riordan, C. R., Lachapelle, A., Delgado, C., Parkes, V., Wadsworth, S. C., Smith, A. E., and Francis, G. E. (1999) PEGylation of adenovirus with retention of infectivity and protection from neutralizing antibody *in vitro* and *in vivo*. *Hum. Gene Ther.* **10,** 1349–1358
20. Hashizume, H., Baluk, P., Morikawa, S., McLean, J. W., Thurston, G., Roberge, S., Jain, R. K., and McDonald, D. M. (2000) Openings between defective endothelial cells explain tumor vessel leakiness. *Am. J. Pathol.* **156,** 1363–1380
21. Jain, R. K. (2001) Delivery of molecular and cellular medicine to solid tumors. *Adv. Drug. Deliv. Rev.* **46,** 149–168
22. Bergelson, J. M., Cunningham, J. A., Droguett, G., Kurt-Jones, E. A., Krithivas, A., Hong, J. S., Horwitz, M. S., Crowell, R. L., and Finberg, R. W. (1997) Isolation of a common receptor for Coxsackie B viruses and adenoviruses 2 and 5. *Science* **275,** 1320–1323
23. Shayakhmetov, D. M., Eberly, A. M., Li, Z. Y., and Lieber, A. (2005) Deletion of penton RGD motifs affects the efficiency of both the internalization and the endosome escape of viral particles containing adenovirus serotype 5 or 35 fiber knobs. *J. Virol.* **79,** 1053–1061
24. Dechecchi, M. C., Melotti, P., Bonizzato, A., Santacatterina, M., Chilosi, M., and Cabrini, G. (2001) Heparan sulfate glycosaminoglycans are receptors sufficient to mediate the initial binding of adenovirus types 2 and 5. *J. Virol.* **75,** 8772–8780
25. Waddington, S. N., McVey, J. H., Bhella, D., Parker, A. L., Barker, K., Atoda, H., Pink, R., Buckley, S. M., Greig, J. A., Denby, L., Custers, J., Morita, T., Francischetti, I. M., Monteiro, R. Q., Barouch, D. H., van Rooijen, N., Napoli, C., Havenga, M. J., Nicklin, S. A., and Baker, A. H. (2008) Adenovirus serotype 5 hexon mediates liver gene transfer. *Cell* **132,** 397–409
26. Huang, Y. Z., Gao, J. Q., Liang, W. Q., and Nakagawa, S. (2005) Preparation and characterization of liposomes encapsulating chitosan nanoparticles. *Biol. Pharm. Bull.* **28,** 387–390
27. Qiu, C., De Young, M. B., Finn, A., and Dichek, D. A. (1998) Cationic liposomes enhance adenovirus entry via a pathway independent of the fiber receptor and alpha(v)-integrins. *Hum. Gene Ther.* 9, 507–520
28. Lee, E. M., Hong, S. H., Lee, Y. J., Kang, Y. H., Choi, K. C., Choi, S. H., Kim, I. H., and Lim, S. J. (2004) Liposome-complexed adenoviral gene transfer in cancer cells expressing various levels of coxsackievirus and adenovirus receptor. *J. Cancer Res. Clin. Oncol.* **130,** 169–177
29. Clark, P. R., Stopeck, A. T., Brailey, J. L., Wang, Q., McArthur, J., Finer, M. H., and Hersh, E. M. (1999) Polycations and cationic lipids enhance adenovirus transduction and transgene expression in tumor cells. *Cancer Gene. Ther.* **6,** 437–446
30. Yotnda, P., Chen, D. H., Chiu, W., Piedra, P. A., Davis, A., Templeton, N. S., and Brenner, M. K. (2002) Bilamellar cationic liposomes protect adenovectors from preexisting humoral immune responses. *Mol. Ther.* **5,** 233–241
31. Steel, J. C., Cavanagh, H. M., Burton, M. A., Dingwall, D. J., and Kalle, W. H. (2005) Modification of liposomal concentration in liposome/adenoviral complexes allows significant protection of adenoviral vectors from neutralising antibody, *in vitro*. *J. Virol. Methods* **126,** 31–36
32. Ma, Z., Mi, Z., Wilson, A., Alber, S., Robbins, P. D., Watkins, S., Pitt, B., and Li, S. (2002) Redirecting adenovirus to pulmonary endothelium by cationic liposomes. *Gene Ther.* **9,** 176–182
33. Parker, A. L., Fisher, K. D., Oupicky, D., Read, M. L., Nicklin, S. A., Baker, A. H., and Seymour, L. W. (2005) Enhanced gene transfer activity of peptide-targeted gene-delivery vectors. *J. Drug Target.* **13,** 39–51
34. Croyle, M. A., Chirmule, N., Zhang, Y., and Wilson, J. M. (2002) PEGylation of E1-deleted adenovirus vectors allows significant gene expression on readministration to liver. *Hum. Gene Ther.* **13,** 1887–1900
35. Fisher, K. D., Green, N. K., Hale, A., Subr, V., Ulbrich, K., and Seymour, L. W. (2007) Passive tumour targeting of polymer-coated adenovirus for cancer gene therapy. *J. Drug Target.* **15,** 546–551
36. Singh, R., Al-Jamal, K. T., Lacerda, L., and Kostarelos, K. (2008) Nanoengineering artificial lipid envelopes around adenovirus by self-assembly. *ACS Nano.* **2,** 1040–1050
37. Green, N. K., Herbert, C. W., Hale, S. J., Hale, A. B., Mautner, V., Harkins, R., Hermiston, T., Ulbrich, K., Fisher, K. D., and Seymour, L. W. (2004) Extended plasma circulation time and decreased toxicity of polymer-coated adenovirus. *Gene Ther.* **11,** 1256–1263
38. Klibanov, A. L., Maruyama, K., Torchilin, V. P., and Huang, L. (1990) Amphipathic polyethyleneglycols effectively prolong the circulation time of liposomes. *FEBS Lett.* **268,** 235–237
39. Weissig, V., Whiteman, K. R., and Torchilin, V. P. (1998) Accumulation of protein-loaded long-circulating micelles and liposomes in subcutaneous Lewis lung carcinoma in mice. *Pharm. Res.* **15,** 1552–1556
40. Campbell, R. B., Fukumura, D., Brown, E. B., Mazzola, L. M., Izumi, Y., Jain, R. K., Torchilin, V. P., and Munn, L. L. (2002) Cationic charge determines the distribution of liposomes between the vascular and extravascular compartments of tumors. *Cancer Res.* **62,** 6831–6836
41. Arulsudar, N., Subramanian, N., Mishra, P., Sharma, R. K., and Murthy, R. S. (2003) Preparation, characterisation and biodistribution of 99mTc-labeled liposome encapsulated cyclosporine. *J. Drug Target.* **11,** 187–196
42. Levchenko, T. S., Rammohan, R., Lukyanov, A. N., Whiteman, K. R., and Torchilin, V. P. (2002) Liposome clearance in mice: the effect of a separate and combined presence of surface charge and polymer coating. *Int. J. Pharm.* **240,** 95–102
43. Tao, N., Gao, G. P., Parr, M., Johnston, J., Baradet, T., Wilson, J. M., Barsoum, J., and Fawell, S. E. (2001) Sequestration of adenoviral vector by Kupffer cells leads to a nonlinear dose response of transduction in liver. *Mol. Ther.* **3,** 28–35
44. Russell, W. C. (2000) Update on adenovirus and its vectors. *J. Gen. Virol.* **81,** 2573–2604
45. Kramp, W. J., Six, H. R., Drake, S., and Kasel, J. A. (1979) Liposomal enhancement of the immunogenicity of adenovirus type 5 hexon and fiber vaccines. *Infect. Immun.* **25,** 771–773
46. Hama, S., Akita, H., Ito, R., Mizuguchi, H., Hayakawa, T., and Harashima, H. (2006) Quantitative comparison of intracellular trafficking and nuclear transcription between adenoviral and lipoplex systems. *Mol. Ther.* **13,** 786–794
47. Chuah, M. K., Collen, D., and VandenDriessche, T. (2003) Biosafety of adenoviral vectors. *Curr. Gene. Ther.* **3,** 527–543
48. Ni, S., Bernt, K., Gaggar, A., Li, Z. Y., Kiem, H. P., and Lieber, A. (2005) Evaluation of biodistribution and safety of adenovirus vectors containing group B fibers after intravenous injection into baboons. *Hum. Gene Ther.* **16,** 664–677
49. Chen, M. Y., Hoffer, A., Morrison, P. F., Hamilton, J. F., Hughes, J., Schlageter, K. S., Lee, J., Kelly, B. R., and Oldfield, E. H. (2005) Surface properties, more than size, limiting convective distribution of virus-sized particles and viruses in the central nervous system. *J. Neurosurg.* **103,** 311–319
50. Wickham, T. J. (2000) Targeting adenovirus. *Gene Ther.* **7,** 110–114
51. Yuan, F., Dellian, M., Fukumura, D., Leunig, M., Berk, D. A., Torchilin, V. P., and Jain, R. K. (1995) Vascular permeability in a human tumor xenograft: molecular size dependence and cutoff size. *Cancer Res.* **55,** 3752–3756
52. Fukuhara, H., Hayashi, Y., Yamamoto, N., Fukui, T., Nishikawa, M., Mitsudo, K., Tohnai, I., Ueda, M., Mizuno, M., and Yoshida, J. (2003) Improvement of transduction efficiency of recombinant adenovirus vector conjugated with cationic liposome for human oral squamous cell carcinoma cell lines. *Oral Oncol.* **39,** 601–609
53. Lee, S. G., Yoon, S. J., Kim, C. D., Kim, K., Lim, D. S., Yeom, Y. I., Sung, M. W., Heo, D. S., and Kim, N. K. (2000) Enhancement of adenoviral transduction with polycationic liposomes *in vivo*. *Cancer Gene Ther.* **7,** 1329–1335

54. Steel, J. C., Cavanagh, H. M., Burton, M. A., Abu-Asab, M. S., Tsokos, M., Morris, J. C., and Kalle, W. H. (2007) Increased tumor localization and reduced immune response to adenoviral vector formulated with the liposome DDAB/DOPE. *Eur. J. Pharm. Sci.* **30,** 398–405
55. Fasbender, A., Zabner, J., Chillon, M., Moninger, T. O., Puga, A. P., Davidson, B. L., and Welsh, M. J. (1997) Complexes of adenovirus with polycationic polymers and cationic lipids increase the efficiency of gene transfer *in vitro* and *in vivo*. *J. Biol. Chem.* **272,** 6479–6489
56. Meunier-Durmort, C., Picart, R., Ragot, T., Perricaudet, M., Hainque, B., and Forest, C. (1997) Mechanism of adenovirus improvement of cationic liposome-mediated gene transfer. *Biochim. Biophys. Acta* **1330,** 8–16
57. Moura, S. P., and Carmona-Ribeiro, A. M. (2005) Biomimetic particles: optimization of phospholipid bilayer coverage on silica and colloid stabilization. *Langmuir* **21,** 10160–10164
58. Kunisawa, J., Masuda, T., Katayama, K., Yoshikawa, T., Tsutsumi, Y., Akashi, M., Mayumi, T., and Nakagawa, S. (2005) Fusogenic liposome delivers encapsulated nanoparticles for cytosolic controlled gene release. *J. Control. Release* **105,** 344–353
59. Krasnici, S., Werner, A., Eichhorn, M. E., Schmitt-Sody, M., Pahernik, S. A., Sauer, B., Schulze, B., Teifel, M., Michaelis, U., Naujoks, K., and Dellian, M. (2003) Effect of the surface charge of liposomes on their uptake by angiogenic tumor vessels. *Int. J. Cancer* **105,** 561–567
60. Litzinger, D. C., Brown, J. M., Wala, I., Kaufman, S. A., Van, G. Y., Farrell, C. L., and Collins, D. (1996) Fate of cationic liposomes and their complex with oligonucleotide *in vivo*. *Biochim. Biophys. Acta* **1281,** 139–149
61. Le Masne de Chermont, Q., Chaneac, C., Seguin, J., Pelle, F., Maitrejean, S., Jolivet, J. P., Gourier, D., Bessodes, M., and Scherman, D. (2007) Nanoprobes with near-infrared persistent luminescence for *in vivo* imaging. *Proc. Natl. Acad. Sci. U. S. A.* **104,** 9266–9271
62. Wolff, G., Worgall, S., van Rooijen, N., Song, W. R., Harvey, B. G., and Crystal, R. G. (1997) Enhancement of *in vivo* adenovirus-mediated gene transfer and expression by prior depletion of tissue macrophages in the target organ. *J. Virol.* **71,** 624–629
63. Snoeys, J., Mertens, G., Lievens, J., van Berkel, T., Collen, D., Biessen, E. A. L., and De Geest, B. (2006) Lipid emulsions potently increase transgene expression in hepatocytes after adenoviral transfer. *Mol. Ther.* **13,** 98–107
64. Gabizon, A. A., Shmeeda, H., and Zalipsky, S. (2006) Pros and cons of the liposome platform in cancer drug targeting. *J. Liposome Res.* **16,** 175–183
65. Roux, E., Passirani, C., Scheffold, S., Benoit, J. P., and Leroux, J. C. (2004) Serum-stable and long-circulating, PEGylated, pH-sensitive liposomes. *J. Control. Release* **94,** 447–451
66. Green, N. K., and Seymour, L. W. (2002) Adenoviral vectors: systemic delivery and tumor targeting. *Cancer Gene Ther.* **9,** 1036–1042
67. Richardson, V. J., Jeyasingh, K., Jewkes, R. F., Ryman, B. E., and Tattersall, M. H. (1978) Possible tumor localization of Tc-99m-labeled liposomes: effects of lipid composition, charge, and liposome size. *J. Nucl. Med.* **19,** 1049–1054
68. Yamashita, M., Ino, A., Kawabata, K., Sakurai, F., and Mizuguchi, H. (2007) Expression of coxsackie and adenovirus receptor reduces the lung metastatic potential of murine tumor cells. *Int. J. Cancer* **121,** 1690–1696

Received for publication February 1, 2008.
Accepted for publication May 8, 2008.